Integral Field Spectroscopy of Local Luminous Compact Blue Galaxies: NGC7673 a case study

A. Castillo-Morales[1], J. Gallego[1], J. Pérez-Gallego[2], R. Guzmán[2], C. Garland[3], D.J. Pisano[4], F. Castander[5], N. Gruel[2], J. Zamorano[1]

Abstract Luminous Compact Blue Galaxies (LCBGs) are high surface brightness starburst galaxies bluer than a typical SBc and with typical luminosities $\approx$ L*, which are undergoing a major burst of star formation. LCBGs are the closest counterparts to the large population of starburst galaxies observed at high redshift, including Lyman-break galaxies at z$\approx$2. However, because LCBGs are very rare in the nearby Universe, their properties are still largely unknown. We have selected a representative sample of LCBGs from the SDSS and UCM databases which, although small, provides an excellent reference for comparison with current and future surveys of similar starbursts at high-z. We are carrying out a 3D optical and radio spectroscopic study of this LCBG sample, including spatially resolved maps of kinematics, extinction, SFR and metallicity. This will allow us to characterize their star formation history and mass assembly, and the role of mergers and supernova galactic winds. Here we show our results of this comprehensive multiwavelength study for NGC 7673, a prototypical LCBG in the nearby Universe.

1 Sample Selection and Observations

LCBGs are selected from the SDSS and UCM databases according to observational criteria that ensure that LCBGs we observe locally are analogous to those observed in deep images of distant galaxy populations: MB$<$-18.5, and SBe$<$21 mag arcsec^{-1}, and B-V$<$0.6 mag. These galaxies (sample of 40 galaxies) were observed with PPAK, an optical integral field unit at the 3.5m Telescope of CAHA, which provides both good spatial and spectral resolution(we use two spectral configurations 300 lines/mm and 1200 lines/mm . In concert with data from other wavelengths, these data allows us to comprehensively study the history of star formation and the mass assembly process in these galaxies.

(1) Universidad Complutense de Madrid (Spain), e-mail: acm@astrax.fis.ucm.es · (2) University of Florida (USA) · (3) Castleton State College, Vermont (USA) · (4) National Radio Astronomy Observatory, Green Bank (USA) · (5) Instituto de Estudios Espaciales de Cataluña (Spain)

2 Data Reduction and Analysis

The data reduction consists of three main steps (1) the standard reduction of two-dimensional fiber spectra using IRAF environment, R3D and E3D software following [7], (2) the line fitting procedure and (3) the generation of maps of spectral features from the calibrated spectra. For each spectrum in the datacube, different quantities such as the total flux, equivalent widths, radial velocities and velocity dispersions were measured by fitting single Gaussians functions to the observed emission-line profiles. To obtain an accurate value of the Balmer emission lines fluxes, we take into account the presence of an underlying stellar absorption . This stellar absorption is clearly more important in the central star formation clump (see map of Hβ absorption equivalent width in Fig. 1) and affect considerably the calculation of quantities such as the extinction. To solve this problem, two Gaussians functions are fitted in those cases were the absorption wings are visible. We use for this purpose the v1200 datacube whose spectral resolution allows us to better fit the absorption wings in Hβ Balmer line (see some examples of fitted spectra in Fig. 1). When the integrated galaxy spectrum is fitted EW_{abs} = 5.0+0.5Å.

3 Results

3.1 Physical Properties

NGC 7673 is a prototypical LCBG at 49 Mpc. This is the first time this galaxy has been fully spectroscopically mapped in the optical. NGC 7673 shows a clumpy structure with starforming knots in the galactic disk that accounts for a SFR between 3.3 and 5.2 $M_{\odot}$/yr mainly associated to older clump A, and clumps B and C ([6]) (see Fig. 1). We derive a total SFR of $6.3 \pm 0.5 M_{\odot}/yr$ (see Fig. 1 for the SFR density map) from the Hα extinction-corrected emission fluxes. The total colour excess E(B-V) map computed from the Balmer line ratio Hα/Hβ is shown in Fig. 1 . The E(B-V) values are in agreement with those found in [6] where the cluster reddening (including the Galactic extinction 0.04 mag) found is lower than 0.44 mag with the large majority of clusters in this galaxy having $0 \leq E(B-V) \leq 0.29$ mag. [2] computed SFR from IRAS fluxes and obtained for this galaxy SFR=5.5 $M_{\odot}$/yr.

A precise measurement of the weak auroral forbidden emission line [OIII]l4363 give an accurate determination of oxygen abundance in gaseosus ionized nebulae. The SNR of this emission line is low for almost all the spectra in our datacube except in clump B where the stellar absorption wings in Hγ are almost absent an allows a better determination of [OIII]λ4363 emission flux. This emission is used to determine the oxygen abudance at least in this region B, given an abundance of 12+log(O/H)=7.98 ± 0.15 (1/5 $Z_{\odot}$). R23 method based in the line ratios: F([OII]λ3727+F([OIII]λ4959,5007)/F(Hβ) give us an estimation of the oxygen abundance very similar in region B and a value of 12+log(O/H)=8.14$\pm$0.25 for the integrated spectrum. We have computed different emission line ratios maps

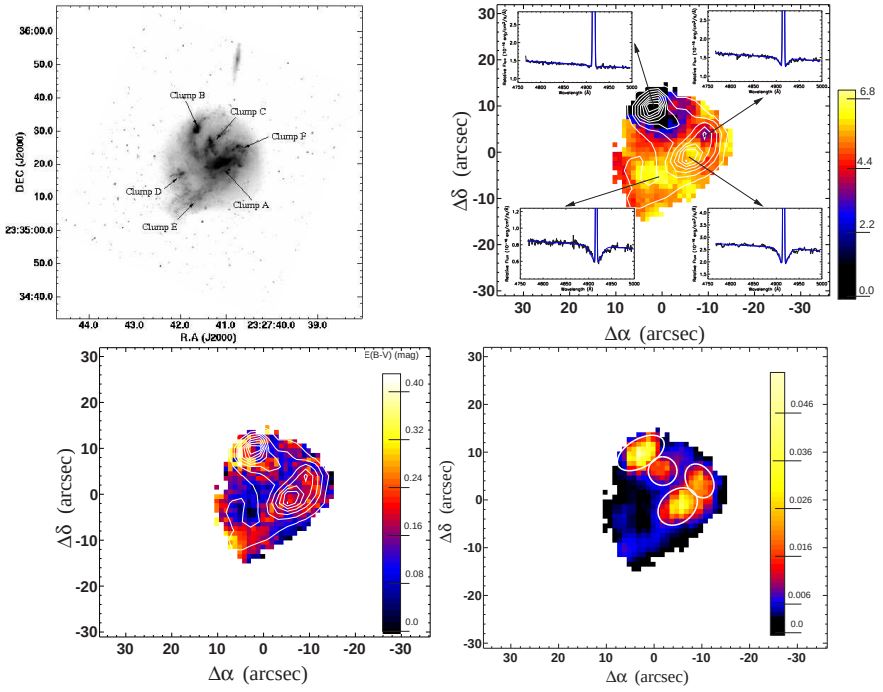

Fig. 1 Top left: NGC 7673 F555W WFPC2/HST image with the main clumps from [1] located. Top right: Hβ absorption equivalent width map copmuted from the double gaussian fit method. Contours from Hα emission are overlaid in white colour. Different fitted spectra are shown to illustrate the method. Bottom left: PPAK total colour excess map computed from the Balmer emission lines ratio F(Hα)/F(Hβ). Bottom right: Star formation density map displayed in logarithmic scale computed from reddening-corrected Hα flux map (colorbar units are $M_{\odot}/yr/arcsec^2$).

as [OIII]λ5007/Hβ,[NII]/Hα, [SII]/Hα to study the possible presence of an AGN, shocks in this galaxy, but all the regions are compatible with HII region.

3.2 Kinematics

The optical velocity map of the galaxy (Fig.2) derived from the centroids of the Hα emission line shows an asymmetric velocity field probably due to the effects of a past minor merger as suggested by [4]. The optical velocity map resembles the HI velocity map both in overall appearance and velocity range ($\approx$100 km/s). The inferred vrot translates into a dynamical mass within R_{eff} (R_{eff}=1.9 kpc) of at least 2.2x10^9 $M_{\odot}$, consistent with the 2.5x10^{10} $M_{\odot}$ inferred by [5] within R_{HI} ($R_{HI} \approx 4.5 R_{eff}$), assuming in both cases an inclination of 45. The distribution of

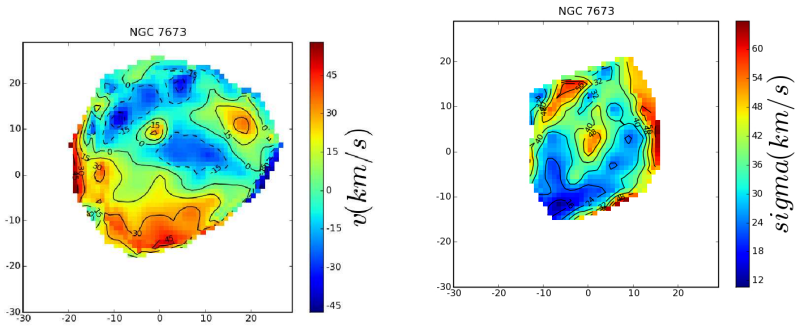

Fig. 2 Left: PPAK Hα velocity map derived using v300 configuration shows asymmetric velocity field probably due to the effects of a past minor merger. Right: PPAK [OIII]λ5007 velocity dispersion map using v1200 configuration. North is to the top and east is to the left.

the HI resembles that of the ionized gas, while the H2 distribution, inferred from CO observations, concentrates in a region along clump A (Fig. X in [3]). This might suggest that both B and C clumps are quenching. At the current SFR the HI gas still present in NGC 7673 would be exhausted in about 2 Gyr. Furthermore, it is interesting to notice the presence of a kinematically decoupled component at the position of clump B. This component may be both moving at a speed of 60km/s, and smaller than 200 pc according to the spatial resolution of our data and the dithering technique used to gather them. The velocity dispersion in NGC 7673 (Fig. 2) peaks around the center of the field of view, σ=54 km/s between clumps A and C, which roughly coincides with its photometric and geometric center. Two further elongated peaks as intense as the central one can be found to the northeast and northwest of the galaxy.

The complete analysis of these data will be found in Pérez-Gallego et al. 2008 and Castillo-Morales et al. 2008.

References

1. Duflot-Augarde, R. & Alloin, D.: A&A **112**, p257 (1982)
2. Garland, C. A., Williams, J. P., Pisano, D. J.,,Guzm'an, R., Castander, F. J. and Brinkmann, J. ApJ **624**, p714 (2005)
3. Garland, C. A. Pisano, D. J., Williams, J. P., Guzm'an, R., Castander, F. J. and Sage, Leslie J. ApJ **671**, p310 (2005)
4. Homeier, N. L. and Gallagher, J. S. ApJ **522**, p199 (1999)
5. Pisano, D. J., Kobulnicky, Henry A., Guzm'an, R., Gallego, J.; Bershady, M. A. AJ **122**, p1194 (2001)
6. Pasquali, A. & Castangia, P. MNRAS **385**, p468 (2008)
7. Sanchez, S.F. Astron. Nachrichten **327**, p850 (2006)